AMERICAN SOCIETY FOR MICROBIOLOGY | Journal of Virology

Rationally Designed Immunogens Targeting HIV-1 gp120 V1V2 Induce Distinct Conformation-Specific Antibody Responses in Rabbits

Xunqing Jiang,[a] Max Totrov,[b] Wei Li,[c] Jared M. Sampson,[a] Constance Williams,[d] Hong Lu,[e] Xueling Wu,[e] Shan Lu,[c] Shixia Wang,[c] Susan Zolla-Pazner,[f] Xiang-Peng Kong[a]

Department of Biochemistry and Molecular Pharmacology, New York University School of Medicine, New York, New York, USA[a]; Molsoft, LLC, San Diego, California, USA[b]; Department of Medicine, University of Massachusetts Medical School, Worcester, MA, USA[c]; Department of Pathology, New York University School of Medicine, New York, New York, USA[d]; Aaron Diamond AIDS Research Center, New York, New York, USA[e]; Division of Infectious Diseases, Icahn School of Medicine at Mount Sinai, New York, New York, USA[f]

ABSTRACT

The V1V2 region of HIV-1 gp120 harbors a major vulnerable site targeted by a group of broadly neutralizing monoclonal antibodies (MAbs) such as PG9 through strand-strand recognition. However, this epitope region is structurally polymorphic as it can also form a helical conformation recognized by RV144 vaccine-induced MAb CH58. This structural polymorphism is a potential mechanism for masking the V1V2 vulnerable site. Designing immunogens that can induce conformation-specific antibody (Ab) responses may lead to vaccines targeting this vulnerable site. We designed a panel of immunogens engrafting the V1V2 domain into trimeric and pentameric scaffolds in structurally constrained conformations. We also fused V1V2 to an Fc fragment to mimic the unconstrained V1V2 conformation. We tested these V1V2-scaffold proteins for immunogenicity in rabbits and assessed the responses by enzyme-linked immunosorbent assay (ELISA) and competition assays. Our V1V2 immunogens induced distinct conformation-specific Ab responses. Abs induced by structurally unconstrained immunogens reacted preferentially with unconstrained V1V2 antigens, suggesting recognition of the helical configuration, while Abs induced by the structurally constrained immunogens reacted preferentially with constrained V1V2 antigens, suggesting recognition of the β-strand conformation. The Ab responses induced by the structurally constrained immunogens were more broadly reactive and had higher titers than those induced by the structurally unconstrained immunogens. Our results demonstrate that immunogens presenting the different structural conformations of the gp120 V1V2 vulnerable site can be designed and that these immunogens induce distinct Ab responses with epitope conformation specificity. Therefore, these structurally constrained V1V2 immunogens are vaccine prototypes targeting the V1V2 domain of the HIV-1 envelope.

IMPORTANCE

The correlates analysis of the RV144 HIV-1 vaccine trial suggested that the presence of antibodies to the V1V2 region of HIV-1 gp120 was responsible for the modest protection observed in the trial. In addition, V1V2 harbors one of the key vulnerable sites of HIV-1 Env recognized by a family of broadly neutralizing MAbs such as PG9. Thus, V1V2 is a key target for vaccine development. However, this vulnerable site is structurally polymorphic, and designing immunogens that present different conformations is crucial for targeting this site. We show here that such immunogens can be designed and that they induced conformation-specific antibody responses in rabbits. Our immunogens are therefore prototypes of vaccine candidates targeting the V1V2 region of HIV-1 Env.

The HIV-1 envelope (Env) complex of glycoproteins gp120 and gp41 is the target for neutralizing antibodies (nAbs) induced in HIV-1-infected patients and for HIV/AIDS vaccine development (1, 2). Glycoprotein gp120 has been conventionally divided into five variable and five conserved regions (3), and the region of the first and second variable loops (V1V2) is the most diverse region of Env in both sequence and length (4). However, recent data have shown that V1V2 can form, in the structurally constrained scaffolded V1V2 or the stabilized BG505 SOSIP.664 trimer, a unique five-stranded β-barrel structure with strands A, B, C, C′, and D (5, 6). In the trimer context, the V1V2 domain is located at the apex of the Env trimer, and the three V1V2 regions in the trimer join together at the center to form a top layer of the Env complex (5, 7–9). This layer can shield the coreceptor binding sites as well as partially occlude the third variable region (V3); it can also make large movements upon CD4 receptor binding to expose the coreceptor binding sites (5, 10, 11). V1V2 also harbors a putative integrin-binding site that may also mediate Env binding to host cells (12–14). One such site, the tripeptide LD(I/V) motif at amino acid positions 179 to 181 (HxB2 numbering) (15), is located at the beginning of the C′ strand in the β-barrel (6).

The spatial apex location of V1V2 on the Env spike makes it a natural target for the human immune system. HIV-infected individuals can make cross-reactive V1V2 Abs, and many human anti-V1V2 monoclonal antibodies (MAbs) have been isolated (16–25). Epitopes for some of these MAbs have been characterized and

Received 14 July 2016 **Accepted** 23 September 2016

Accepted manuscript posted online 5 October 2016

Citation Jiang X, Totrov M, Li W, Sampson JM, Williams C, Lu H, Wu X, Lu S, Wang S, Zolla-Pazner S, Kong X-P. 2016. Rationally designed immunogens targeting HIV-1 gp120 V1V2 induce distinct conformation-specific antibody responses in rabbits. J Virol 90:11007–11019. doi:10.1128/JVI.01409-16.

Editor: G. Silvestri, Emory University

Address correspondence to Xiang-Peng Kong, xiangpeng.kong@med.nyu.edu.

For a companion article on this topic, see doi:10.1128/JVI.01403-16.

were recently classified into three major types: V2i, V2p, and V2q (26, 27). The V2i type is defined by a panel of human MAbs, including 830A, 697-D, and 2158 (17, 26–30). Extensive immunological, mutagenesis, and structural data have shown that the V2i epitopes overlap the LD(I/V) integrin-binding site, and Abs of this family recognize discontinuous regions in V1V2 (6, 26–28). The V2p type is defined by human MAbs CH58 and CH59 isolated from a vaccinee of the phase III RV144 human vaccine trial (23, 31, 32). Monoclonal Abs CH58 and CH59 react with V2 peptides, indicating that the V2p epitopes are structurally unconstrained and have a helical or helical-coil structure (23). The V2q type was defined by quaternary neutralizing epitope MAbs including PG9 and PG16 (19). Crystal structures of PG9 and PG16 in complex with engineered V1V2 scaffolds have shown that these MAbs recognize a region in strand C of V1V2, via a strand-strand interaction, as well as two N-linked glycans using the head of the long complementarity-determining region (CDR) H3 harbored by these V2q MAbs (33, 34). In the V1V2 scaffolds used to crystallize these MAbs, the V1V2 from ZM109 or CAP45 [V1V2(ZM109) or V1V2(CAP45), respectively] is grafted into a β-hairpin region in the protein G B1 domain (Protein Data Bank [PDB] accession number 1FD6) so that the V1V2 is structurally constrained to maintain the conformation found in the trimeric apex (5). Although the protein regions of the V2q epitopes overlaps that of the V2p epitopes, the structures of the former have a β-strand conformation while those of the latter have a helical conformation. The V2p MAbs have weak and very restricted neutralizing activities (23), while the V2q-specific MAbs PG9 and PG16 have been shown to neutralize greater than 70% of virus strains tested (19). Thus, the V2q epitope region is a major site of vulnerability on Env; designing immunogens that can induce Ab responses targeting this conformation has not yet been accomplished.

Data from the correlates analysis of the human clinical vaccine trial RV144, the only human vaccine trial with moderate but significant efficacy against HIV-1 acquisition, have demonstrated that vaccine-induced IgG Abs targeting V1V2 inversely correlated with the risk of infection (35), and immunologic data delineated the specificity and cross-reactivity of these Abs (36, 37). The Abs induced by the vaccine reacted with a murine leukemia virus (MuLV) V1V2 gp70 fusion protein, a reagent recognized by the V2i Abs (28). There was no evidence of the elicitation of V2q Abs by the RV144 vaccine in that little neutralizing activity was detected, and neutralization was not associated with reduced infection rates (35, 38). A sieve analysis that compared the V1V2 sequences of viruses from placebo and those from vaccine recipients identified two positions of immune pressure on the virus in V2, residues 169 and 181, supporting the hypothesis that V1V2 Abs correlated with the reduced risk of infection (39). These findings suggest that V1V2 can serve as an important target for HIV vaccine development, but the modest efficacy of RV144 indicates the need for a more efficacious vaccine.

Designing immunogens targeting various epitopes of V1V2 and dissecting Ab responses targeting the three epitope types in animal models will help further improve upon current vaccine candidates. We show here that immunogens presenting various representations of the V1V2 epitopes can be rationally designed and that these different immunogens induce distinct Ab responses targeting the particular defined epitopes within this region. These results provide a proof of principle that vaccine candidates targeting the V1V2 vulnerable sites can be rationally designed.

MATERIALS AND METHODS

Ethics statement. Rabbit experiments were performed according to the guidelines of the Animal Welfare Act at the University of Massachusetts Medical School in its animal facility, which is fully accredited by AAALAC International with a current Animal Welfare Assurance on file. The immunization protocol was reviewed and approved by the Institutional Animal Care and Use Committees of both the University of Massachusetts Medical School and the New York University School of Medicine.

Design of trimeric V1V2 scaffolds. Two trimeric V1V2-scaffold immunogens, V1V2(ZM53)-2J9C and V1V2(ZM109)-2F5K, based on the structures of PDB accession numbers 2J9C and 2F5K, respectively, were designed using the internal coordinate mechanics (ICM) molecular modeling environment (40). We have implemented a pipeline of filters to screen the PDB (http://www.rcsb.org/pdb/) for scaffolds with desired structural features. Symmetric homotrimeric structures were extracted from the PDB. Within each structure, β-hairpins (if present) were identified. Each β-hairpin was checked for surface exposure so that a domain grafted on it could potentially extend into open space without colliding with the scaffold. For each hairpin, its position and orientation with respect to the 3-fold axis of the trimeric assembly were assessed in terms of distance from the trimer axis and two angles (Fig. 1).

Target parameters inferred from the approximate reconstruction of the V1V2 domain position within the trimer were as follows: the center mass of the residue pair (Ala125 and Gln197) immediately preceding the disulfide (Cys126 and Cys196) that delimits the V1V2 domain was ~12 Å from the trimer axis, and the vector of the β-hairpin direction was tilted ~20° both outwards and clockwise around the axis (when viewed from above the trimer apex). Scaffolds that had these three parameters closest to the target were further evaluated by superimposing N- and C-terminal strands of the V1V2 domain structure onto corresponding strands of the scaffold hairpin to create a simple model of the graft-scaffold construct, which was assessed for clashes between the V1V2 domain and the scaffold or between the V1V2s themselves. Finally, complete models were built for the best candidates and energy minimized, and final scaffold selection was made upon visual inspection of the models.

TTB-based immunogen. A crystal structure of typhoid toxin complex (PDB accession number 4K6L) was used to identify a disulfide bond at the C terminus of subunit B that is suitable for insertion of the V1V2 domain (41). A small loop between residues Cys128 and Cys133 in typhoid toxin subunit B (TTB) was replaced with V1V2 amino acids between Cys126 and Cys196 of ZM109 gp120. The structure of V1V2 in the PG9 complex was used to model the scaffolded pentamer, which showed that there were no clashes between the V1V2 regions in the pentamer (Fig. 1D). This construct is named V1V2(ZM109)-TTB.

Fc-linked immunogens. Two types of Fc-linked immunogens were constructed based on the available V1V2 scaffolds by linking them with the rabbit Fc fragment consisting of the heavy chain hinge and the CH2 and CH3 regions. The first type, V1V2(ZM109)-1FD6-Fc, based on the 1FD6-scaffolded V1V2 used in crystallizing V2q MAbs (33, 34), is structurally constrained. The second type, represented by V1V2(1086)-Fc and V1V2(ZM109)-Fc, based on the V1V2-tags protein (23), is structurally unconstrained. The rabbit Fc gene was first cloned into the XbaI/BamHI sites of the mammalian expression vector pVRC8400 (42), and an NheI site was engineered preceding the rabbit Fc gene, located in a spacer between the genes of the V1V2 domain or scaffold and Fc. V1V2(ZM109)-1FD6, V1V2(1086), or V1V2(ZM109) was cloned into the EcoRV/NheI sites of the modified expression vector pVRC8400.

Production of V1V2 immunogens. Gene constructs were codon optimized for mammalian cell expression and synthesized by commercial vendors with a secretion signal, and, for non-Fc linked constructs, a C-terminal human rhinovirus (HRV) 3C protease cleavage site, an 8×His tag, and a Strep-Tag II. They were then cloned into the modified expression vector pVRC8400 (kindly provided by the Vaccine Research Center, National Institutes of Health) (42). Plasmid DNAs encoding these immunogens were transiently transfected into HEK293S GnTI$^{-/-}$ cells (43),

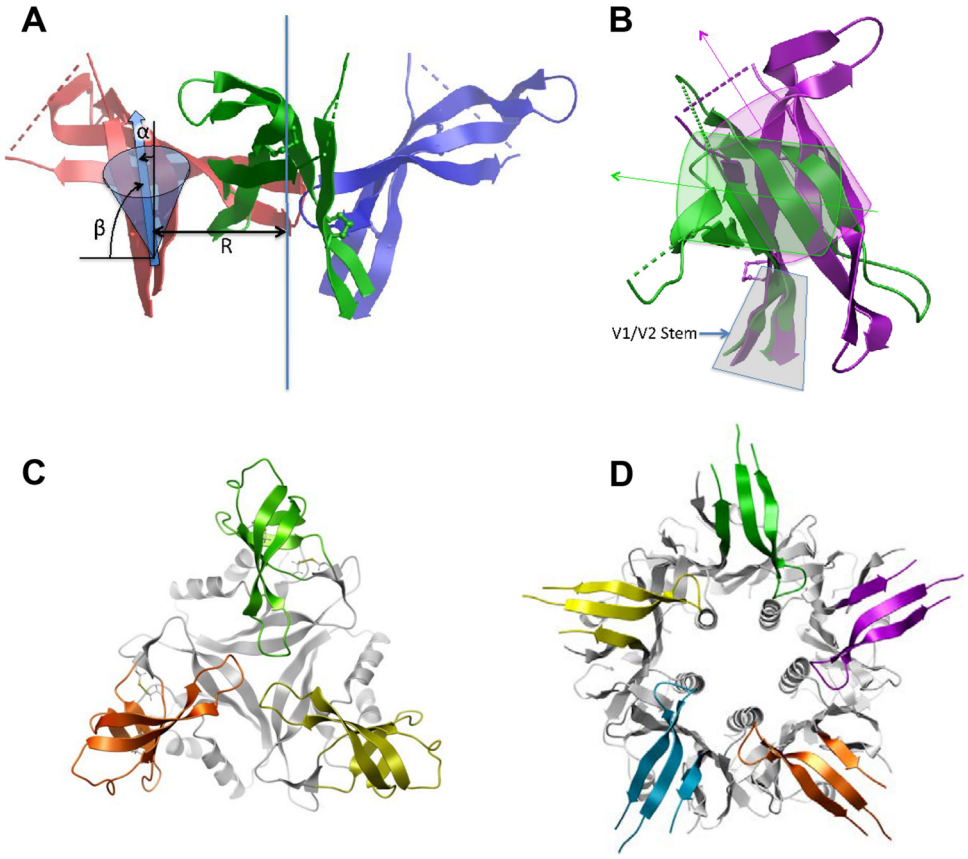

FIG 1 Designing of V1V2 immunogens. (A) Geometric parameters of the β-hairpin orientation of the V1V2 stem used for scaffold filtering. The 3-fold axis (the vertical blue line) of the trimer, the distance (R) of the V1V2 stem from the axis, and tilting angles (α and β) of the V1V2 stem are illustrated. (B) Differences in stem orientation between V1V2 domain complexes with MAb PG9 (magenta) and MAb 830A (green). Stem strands (highlighted in gray) are superimposed, β-barrels and their axes are indicated schematically as cylinders, and arrows highlight the change in barrel orientation. (C) A top view of V1V2(ZM53)-2J9C. The trimeric scaffold (PDB accession number 2J9C) is shown in gray while the three V1V2s, based on the MAb 830A complexed structure, are shown in green, orange, and gold. (D) A top view of V1V2(ZM109)-TTB. The typhoid toxin subunit B (TTB) pentamer is shown in gray while the V1V2 inserts, shown here as the PG9-bound form, are colored. Note that the V1V2s are placed on top of the pentamer without any hindrance against each other.

cultured in Erlenmeyer flasks using 15 to 25% of the nominal volume, and rotated at 110 to 130 rpm under standard humidified conditions (37°C and 5% CO_2). Cells were allowed to secrete the V1V2 immunogens for 72 h. For V1V2(ZM53)-2J9C, V1V2(ZM53)-2F5K, and V1V2(ZM109)-TTB, cell supernatants were concentrated, filtered, and loaded onto Ni-nitrilotriacetic acid (NTA) beads, and proteins were eluted with 600 mM imidazole. For V1V2(ZM109)-1FD6-Fc, V1V2(1086)-Fc, and V1V2(ZM109)-Fc, cell supernatants were concentrated, filtered, and loaded onto protein A columns; proteins were eluted with citric acid. The immunogens were flash frozen and stored at −80°C. The antigenicity of the V1V2-scaffold proteins was tested by ELISA with various human monoclonal antibodies.

Chemical conjugation of V1V2(ZM109)-1FD6 and CTB. Purified cholera toxin subunit B (CTB; Sigma-Aldrich) and V1V2(ZM109)-1FD6 were chemically conjugated using the heterobifunctional cross-linker *N*-succinimidyl 3-(2-pyridyldithio) propionate (SPDP; Thermo Scientific). One milligram of V1V2(ZM109)-1FD6 (2 mg/ml in phosphate-buffered saline [PBS]) was incubated with SPDP (final concentration, 0.6 mM) for 1 h at room temperature to add pyridyl disulfide groups to the primary amines of the protein. The reaction mixture was then desalted and buffer exchanged to PBS by a size exclusion membrane filter to remove excess reagent and by-products (pyridine 2-thione). Similarly, 1 mg of CTB (2 mg/ml in PBS) was incubated with SPDP (final concentration, 0.6 mM) for 1 h at room temperature and then desalted and buffer exchanged to PBS. Pyridyldithiol-activated CTB was then incubated with dithiothreitol (DTT; 50 mM) for 30 min at room temperature to expose the sulfhydryl groups and then desalted and buffer exchanged to PBS as before. Finally, equal amounts of pyridyldithiol-activated V1V2(ZM109)-1FD6 and sulfhydryl-activated CTB were mixed, followed by incubation at room temperature overnight for conjugation. The conjugated sample was desalted as before and purified by size exclusion chromatography, and the endotoxin content was measured to confirm that there had been no significant contamination during the conjugation process.

Immunization of rabbits. Female New Zealand White rabbits, 8 to 10 weeks old (with a body weight of ~2 kg), were purchased from Harlan Laboratories (Indianapolis, IN) and housed in the animal facility managed by the Department of Animal Medicine at the University of Massachusetts Medical School in accordance with an IACUC-approved protocol. Three to five rabbits were included in each immunization group. For the priming immunizations, all rabbits received codon-optimized gp120.ZM109 DNA in the pJW4303 vector and were immunized at weeks 0, 2, and 4 using a Bio-Rad Helios gene gun (Bio-Rad Laboratories, Hercules, CA). The gp120 DNA vaccine plasmids were applied as a coating onto 1.0-μm gold beads at a ratio of 2 μg of DNA per mg of gold. Each gene gunshot delivered 1 μg of DNA to a total of 36 nonoverlapping sites on the shaved abdominal skin for each DNA immunization. In two of the groups (H3.4 and H3.5) (see Table 3), the rabbits also received protein immunogens at the same time as DNA. For the boosting immunizations, the animals received two doses of either gp120(ZM109) or one of the V1V2-scaffold immunogens at weeks 10 and 14. For all protein immuni-

TABLE 1 Amino acid sequences of the rationally designed immunogens used in rabbit experiments H2 and H3

Name	Amino acid sequence
V1V2(ZM53)-2F5K	PKPKFQEGERVLCFHGPLLYEAKCVKVAILAACVTLNCSKLNNATDGEMKNCSFNATTELRDKKKQVYALFYKLDIVPLD GRNNSSEYRLINCEETVKYFIHYSGWNKNWDEWVPESRVLKYVDTNLQKQRELQKANQEQYAEGKGLEVLFQGPG HHHHHHHHSAWSHPQFEK
V1V2(ZM53)-2J9C	GSMKKVEAIIRPEKLEIVKKALSDAGYVGMTVSEVKGRGVQGGIVERYCVTLNCSKLNNATDGEMKNCSFNATTELRDK KKQVYALFYKLDIVPLDGRNNSSEYRLINCREYIVDLIPKVKIELVVKEEDVDNVIDIICENARTGDPGDGKIFVIPVER VVRVRTKEEGKEALLEHGLEVLFQGPGHHHHHHHHHSAWSHPQFEK
V1V2(ZM109)-TTB	EWTGDNTNAYYSDEVISELHVGQIDTSPYFCIKTVKANGAGTPVVACAVSKQSIWAPSFKELLDQARYFYSTGQSVRIHV QKNIWTYPLFVNTFSANALVGLSSCVKLTPLCVTLNCTSPAAHNESETRVKHCSFNITTDVKDRKQKVNATFYDLDIV PLSSSDNSSNSSLYRLISCNTSTITQACFGPKLEVLFQGPGHHHHHHHHHSAWSHPQFEK
V1V2(ZM109)-1FD6-Fc	MTTFKLAACVTLNCTSPAAHNESETRVKHCSFNITTDVKDRKQKVNATFYDLDIVPLSSSDNSSNSSLYRLISCQTTTTEA VDAATAAKVFKQYANDNGIDGEWTYDDATKTFTVTEGLEVLFQGASGGSKPTCPPPELLGGPSVFIFPPKPKDTLMIS RTPEVTCVVVDVSQDDPEVQFTWYINNEQVRTARPPLREQQFNSTIRVVSTLPIAHQDWLRGKEFKCKVHNKALPAP IEKTISKARGQPLEPKVYTMGPPREELSSRSVSLTCMINGFYPSDISVEWEKNGKAEDNYKTTPAVLDSDGSYFLYSKLS VPTSEWQRGDVFTCSVMHEALHNHYTQKSISRSPGK
V1V2(1086)-Fc	SLKPCVKLTPLCVTLNCTNVKGNESDTSEVMKNCSFKATTELKDKKHKVHALFYKLDVVPLNGNSSSSGEYRLINCNTSA ITQACPKVSGASGGSKPTCPPPELLGGPSVFIFPPKPKDTLMISRTPEVTCVVVDVSQDDPEVQFTWYINNEQVRTARP PLREQQFNSTIRVVSTLPIAHQDWLRGKEFKCKVHNKALPAPIEKTISKARGQPLEPKVYTMGPPREELSSRSVSLTCMI NGFYPSDISVEWEKNGKAEDNYKTTPAVLDSDGSYFLYSKLSVPTSEWQRGDVFTCSVMHEALHNHYTQKSISRSPGK
V1V2(ZM109)-Fc	SLKPCVKLTPLCVTLNCTSPAAHNESETRVKHCSFNITTDVKDRKQKVNATFYDLDIVPLSSSDNSSNSSLYRLISCNTSTIT QACPKVSGASGGSKPTCPPPELLGGPSVFIFPPKPKDTLMISRTPEVTCVVVDVSQDDPEVQFTWYINNEQVRTARPPL REQQFNSTIRVVSTLPIAHQDWLRGKEFKCKVHNKALPAPIEKTISKARGQPLEPKVYTMGPPREELSSRSVSLTCMIN GFYPSDISVEWEKNGKAEDNYKTTPAVLDSDGSYFLYSKLSVPTSEWQRGDVFTCSVMHEALHNHYTQKSISRSPGK

zations, a total of 100 μg of the gp120 protein or an individual V1V2-scaffold protein together with incomplete Freund adjuvant (IFA) was administered intramuscularly (i.m.). Serum samples were collected prior to immunization and 2 weeks after each immunization.

ELISA of V1V2 MAbs and antibodies in sera from immunized rabbits. ELISAs were performed using Immulon 4HBX plates coated with antigens at a concentration of 1 μg/ml and incubated overnight at 4°C. After plates were blocked with PBS with 3% bovine serum albumin (BSA) for 1.5 h, MAbs were added at a concentration of 10 μg/ml. For serial titration of test sera, ELISAs were performed with a starting dilution of 1:100, and individual preimmune sera were used as negative controls. Following a 2-h incubation and three washes with PBS-Tween 20 (0.05%), a 1:2,000 dilution of alkaline phosphatase-conjugated goat anti-rabbit IgG (Southern Biotech) was added. After a 1-h incubation, plates were washed three times with PBS-Tween 20. Alkaline phosphatase substrate (Sigma) was added, and plates were read 30 min later at a wavelength of 405 nm. The endpoint titer for each serum was determined by the last dilution that gave twice the signal of the background reading.

Competition antibody binding assay. A competition ELISA was used to determine epitope specificity, i.e., whether sera from vaccinated animals contained Abs recognizing epitopes similar to the well-characterized Env-specific MAbs PG9, CH58, 697-D, and 830A. Dilutions of sera were preincubated for 10 min at room temperature (RT) in wells of plates (Immulon 4HBX) coated with antigens at a concentration of 1 μg/ml, followed by incubation for 2 h at RT with a biotinylated PG9, CH58, 697-D, or 830A. The concentration for each biotinylated MAb used was predetermined in competition with its nonbiotinylated IgG. Plates were washed with PBS containing 0.02% Tween 20 before incubation (1 h at RT) with a streptavidin–horseradish peroxidase (HRP) reporter reagent (product 21130; Pierce). Plates were read at a wavelength of 450 nm. A reduction in signal reflects the presence of Abs in serum that competed with labeled MAbs for binding to the plate-bound antigen.

Neutralization assays. For detection of neutralizing Abs (nAbs) in rabbit immune sera, clade C MW965 (tier 1A) and ZM109 (tier 1B) pseudoviruses from the standard pseudovirus panels were used (44). A standard TZM.bl pseudovirus neutralization assay was performed (44, 45). Briefly, serial dilutions of heat-inactivated serum were prepared starting at a dilution of 1:10. The serum-pseudovirus mixtures were then incubated with the TZM.bl target cells, and luciferase activity was measured 30 min or 24 h later. Prebleed sera were used as negative controls against each pseudovirus, and all sera were also tested against a negative-control pseudovirus carrying the envelope of murine leukemia virus. The percent neutralization was calculated relative to the effect of the preimmune serum from the same rabbit at the same dilution. All sera were assayed in duplicate in at least two experiments against each virus. The 50%, 80%, and 90% inhibitory dose titers were calculated as the serum dilutions that caused these percentages of reduction in relative luminescence units compared to the level in the virus control wells.

RESULTS

Design and construction of structurally unconstrained and constrained immunogens presenting V1V2 epitope types. We first designed a couple of V1V2 immunogens mimicking the trimeric V1V2 conformation in the stabilized BG505 SOSIP.664 gp140 context (46). Our initial design was based on the structures then available: the low-resolution cryo-electron microscopy (EM) structure of BG505 SOSIP/PG9 complex and a crystal structure of a V1V2-1FD6 scaffold/PG9 complex (33, 47). The latter structure demonstrated that V1V2 could be grafted onto β-hairpins within another protein. We searched the PDB for homotrimeric structures with exposed β-hairpins and suitable spatial parameters for scaffolding V1V2 (Fig. 1A and B). We identified that the trimer of the MRG15 chromo-domain (PDB code 2F5K) has a β-hairpin that would accommodate V1V2 with the orientation present in the SOSIP trimer. We designed a V1V2-scaffold immunogen based on these structures, using the ZM53 sequence that has relatively short V1 and V2 hypervariable loops. The chimeric structure included the complete V1V2 domain with the terminal Cys126 and Cys196 of ZM53 fused at the match points to 2F5K, excluding the turn residues in the original scaffold hairpin; this immunogen is named V1V2(ZM53)-2F5K (Table 1). Meanwhile, we had determined a crystal structure of V1V2(ZM109)-1FD6 in complex with a V2i MAb, 830A, and revealed that the

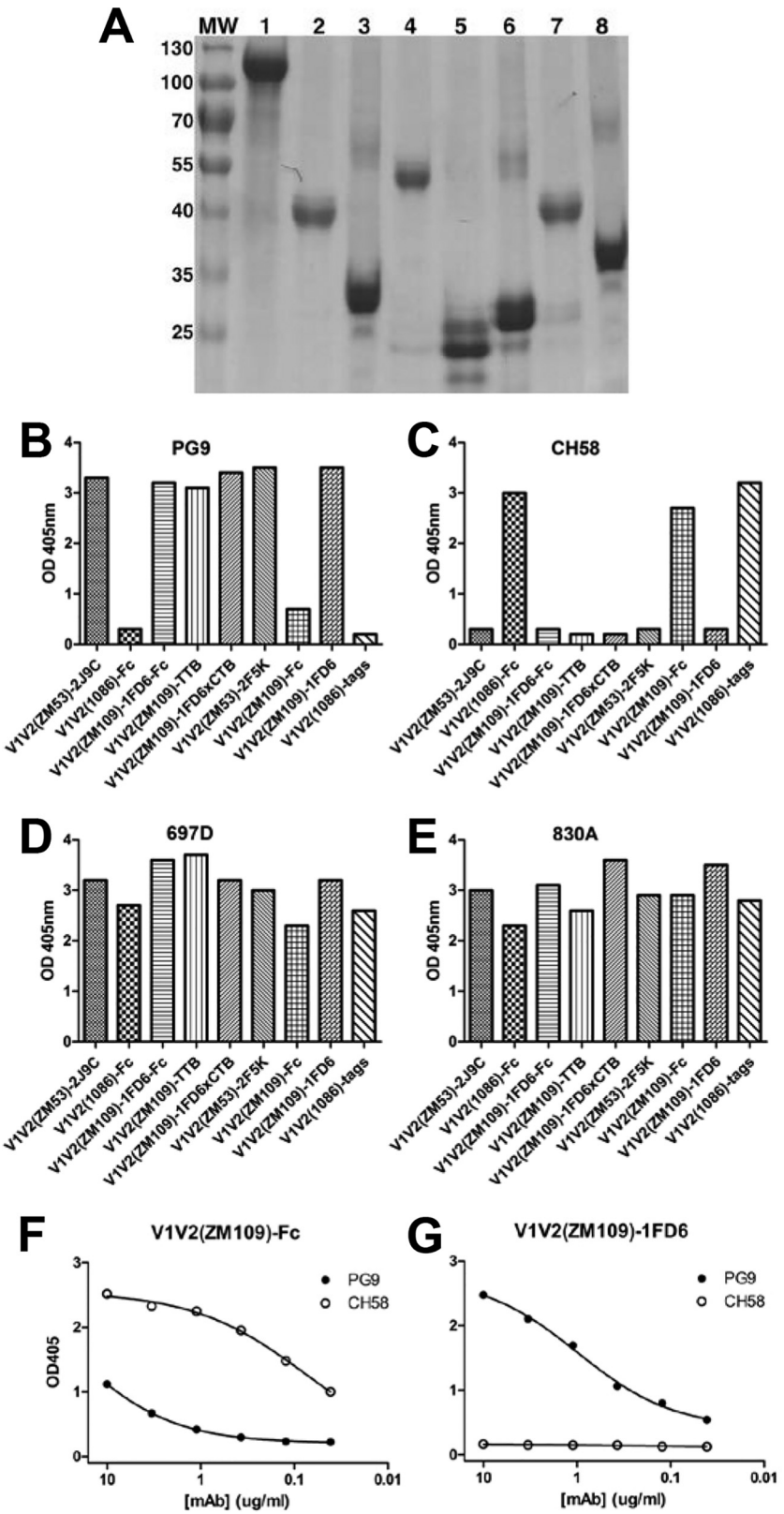

FIG 2 Antigenicity tests of V1V2 immunogens. (A) Electrophoresis of purified immunogens. Isolated molecules were resolved by SDS-PAGE and stained with Coomassie blue. Lanes 1 to 8 are gp120(ZM109), V1V2(1086)-Fc, V1V2(ZM53)-2J9C, V1V2(ZM109)-1FD6-Fc, V1V2(ZM109)-1FD6, V1V2(ZM53)-2F5K, V1V2(ZM109)-Fc, and V1V2(ZM109)-TTB, respectively. Molecular weight (MW) standards (in thousands) are marked on the side. (B to E) Binding of V1V2 immunogens to V2q MAb PG9, V2p MAb CH58, and V2i MAbs 697-D and 830A analyzed by ELISA. Note that in the top two panels, immunogens that bound well to the V2q MAb PG9 bound poorly to the V2p MAb CH58, and vice versa. (F and G) Titration of MAbs PG9 and CH58 to V1V2(ZM109)-1FD6 and V1V2(ZM109)-Fc. Note that although these two V1V2-scaffold antigens have the same V1V2 sequence, the structurally constrained V1V2(ZM109)-1FD6 binds only PG9 while the unconstrained V1V2(ZM109)-Fc binds only CH58. Thus, the V2q epitope type (recognized by PG9) and the V2p epitope type (recognized by CH58) could be selectively presented by the structurally constrained and unconstrained V1V2 immunogens, respectively. OD, optical density.

TABLE 2 Types of epitopes carried by the immunogens and antigens used in this study[a]

Antigen	V2q (reactive with PG9)	V2i (reactive with 697-D and/or 830A)	V2p (reactive with CH58)
V1V2(ZM53)-2J9C	+	+	−
V1V2(1086)-Fc	−	+	+
V1V2(ZM109)-1FD6-Fc	+	+	−
V1V2(ZM109)-TTB	+	+	−
V1V2(ZM109)-1FD6×CTB	+	+	−
V1V2(ZM53)-2F5K	+	+	−
V1V2(ZM109)-Fc	−	+	+
V1V2(ZM109)-1FD6	+	+	−
V1V2(1086)-tags	−	+	+

[a] + and −, presence and absence of the epitope type, respectively.

V1V2 domain can adopt a five-strand β-barrel conformation (6) that is distinct from the four-strand structure observed in complexes with MAbs PG9 and PG16 (33, 34). Remarkably, this change is accompanied by the bending of the V1V2 stem β-strands so that the tilt of the β-barrel with respect to the stem strands is different (Fig. 1B). Search of the PDB showed that the structure of the GlnK1 protein from *Methanococcus jannaschii* (PDB code 2J9C) would be suitable for scaffolding this V1V2 conformation. Thus, we have constructed another trimeric V1V2 scaffold, V1V2(ZM53)-2J9C (Table 1 and Fig. 1C). We produced these trimeric V1V2-scaffold proteins in the HEK293S GnTI$^{-/-}$ cells that produce only high-mannose glycans, which are more homogeneous than complex glycans (43) (Fig. 2A). Antigenicity tests showed that both V1V2(ZM53)-2F5K and V1V2(ZM53)-2J9C could bind PG9 as well as 697-D and 830A; thus, they harbor V2q and V2i epitopes (Fig. 2B to E and Table 2).

As noted above, trimeric arrangement of V1V2 domains in V1V2(ZM53)-2F5K and V1V2(ZM53)-2J9C constructs was based on approximate geometry deduced from low-resolution electron microscopy structures. After the constructs were designed and entered experimental evaluation, high-resolution X-ray structures of SOSIP trimers became available (5, 7). We compared configurations of V1V2 domains in our construct models with the SOSIP structure (PDB accession number 4TVP). We found that the positions of the center of mass of the V1V2 domains deviated by only 1.9Å and 1.6 Å for 2F5K- and 2J9C-based constructs, respectively. The V1V2 domain was also rotated by 18° in the 2F5K-based construct, while in the 2J9C-based construct, the rotation angle reached 96°. Thus, the 2F5K-based construct design is predicted to achieve a V1V2 domain configuration that is significantly closer to the native-like closed spike trimer state. It should be noted that the β-strands connecting the V1V2 domains to the scaffold are likely to be substantially flexible, and therefore domain orientations are expected to sample a range of positions around the modeled ones.

The scaffold molecule V1V2(ZM109)-1FD6 used in crystallization with PG9 and PG16 (33) naturally carries the V2q type of epitopes. However, the molecule is rather small (~25 kDa with glycans) and was not very immunogenic in rabbits (data not shown). We therefore tried to improve its immunogenicity by attaching at its C terminus the rabbit Fc fragment. In the antigenicity test, this bivalent immunogen, V1V2(ZM109)-1FD6-Fc (Table 1), was able to bind PG9 as well as 697-D and 830A (Fig. 2B, D, and E); thus this immunogen harbors the V2q and V2i epitopes (Table 2).

We also constructed two immunogens based on pentameric bacterial toxin B subunits. We had previously tested cholera toxin B subunit (CTB)-based immunogens carrying HIV-1 V3 epitopes and showed that they were highly immunogenic and elicited cross-clade neutralizing Ab responses in rabbits (48–50). To test CTB's effects on V1V2 immunogens, we chemically conjugated the structurally constrained V1V2(ZM109)-1FD6 with the CTB and showed that it preserved the V2q and V2i epitopes in the V1V2 scaffold (Fig. 2B, D, and E). We also created a V1V2-typhoid toxin B subunit (TTB) fusion protein V1V2(ZM109)-TTB (Table 1), taking advantage of the fact that TTB harbors a disulfide bond near its C terminus, which is a naturally suitable place for grafting the disulfide-linked V1V2 domain (PDB accession number 4K6L) (Fig. 1D). Computer modeling showed that the pentameric TTB can host five copies of V1V2 without any structural hindrances (Fig. 1D). Interestingly, V1V2(ZM109)-TTB harbors the structurally constrained V2q and V2i epitopes (Fig. 2B, D, and E) although its pentameric form does not resemble in any way that of V1V2 in the gp120 trimer.

To construct structurally unconstrained V1V2 molecules, we fused the V1V2 domains of clade C strain 1086 or ZM109 to the rabbit Fc (Table 1). Since only the C terminus of the V1V2 (after the V1V2 disulfide bond) is linked to the flexible N terminus of Fc, there are no constraints imposed on the V1V2 β-hairpin stem. Indeed, antigenicity tests showed that V1V2(1086)-Fc and V1V2(ZM109)-Fc were recognized by the V2p MAb CH58 but not by the V2q MAb PG9 (Fig. 2B, C, F, and G); thus, these unconstrained V1V2s harbor the V2p epitopes (Table 2).

These data describe a panel of immunogens that can present the V2q, V2p, and V2i epitopes (Tables 1 and 2). The V2q epitopes can be presented by the immunogens with structurally constrained V1V2s, while the V2p epitopes can be presented by the immunogens with unconstrained V1V2s. In contrast, V2i epitopes can be presented by immunogens with either constrained or unconstrained V1V2s.

DNA prime-protein boost regimen using rationally designed immunogens elicited strong Ab responses targeting gp120 V1V2. To test the immunogenicity of our immunogens, we carried out two rabbit experiments, H2 and H3 (Table 3). In rabbit experiment H2, we tested six immunogens, including the gp120(ZM109) monomer (rabbit group H2.1), the trimeric, structurally constrained V1V2(ZM53)-2J9C (H2.2), the structurally unconstrained V1V2(1086)-Fc (H2.3), the structurally constrained V1V2(ZM109)-1FD6-Fc (H2.4), the pentameric, structurally constrained toxin subunit B-based V1V2(ZM109)-TTB (H2.5), and the structurally constrained cross-linked construct V1V2(ZM109)-1FD6×CTB (H2.6). In this experiment, we used a DNA prime-protein boost regimen (with three consecutive DNA primes followed by three protein boosts) that we had used previously in successfully inducing Ab responses in rabbits (49–51). The DNA priming immunogen was a plasmid DNA encoding monomeric gp120(ZM109). In experiment H3 (Table 3), we tested another trimeric immunogen V1V2(ZM53)-2F5K (group H3.1), repeated the structurally constrained V1V2(ZM109)-1FD6-Fc (H3.2) in comparison with an immunogen with the same V1V2 sequence but structurally unconstrained V1V2(ZM109)-Fc (H3.3). In addition, we tested a new regimen in which animals were primed with the DNA as well as the protein (Table 3) (52), using DNA and

TABLE 3 The design of rabbit studies H2 and H3

Study group	No. of rabbits	Rabbit no.	Prime[a]	Boost[b]
H2.1	3	H2.1.1–H2.1.3	gp120.ZM109 DNA	gp120(ZM109)
H2.2	4	H2.2.1– H2.2.4		V1V2(ZM53)-2J9C
H2.3	4	H2.3.1– H2.3.4		V1V2(1086)-Fc
H2.4	5	H2.4.1– H2.4.5		V1V2(ZM109)-1FD6-Fc
H2.5	5	H2.5.1– H2.5.5		V1V2(ZM109)-TTB
H2.6	4	H2.6.1– H2.6.4		V1V2(ZM109)-1FD6×CTB
H3.1	5	H3.1.1– H3.1.5	gp120.ZM109 DNA	V1V2(ZM53)-2F5K
H3.2	5	H3.2.1– H3.2.5		V1V2(ZM109)-1FD6-Fc
H3.3	5	H3.3.1– H3.3.5		V1V2(ZM109)-Fc
H3.4	5	H3.4.1– H3.4.5	gp120.ZM109 DNA + V1V2(ZM53)-2J9C	V1V2(ZM53)-2J9C
H3.5	5[c]	H3.5.1– H3.5.3, H3.5.5	gp120.ZM109 DNA + V1V2(ZM109)-TTB	V1V2(ZM109)-TTB

[a] For the priming immunizations, the codon-optimized gp120.ZM109 DNA vaccine (36 μg/dose, 1 μg/shot) was delivered by gene gun at weeks 0, 2 and 4, in all groups. In groups H3.4 and H3.5, the rabbits also received V1V2-scaffold protein boosts (100 μg/dose) formulated with IFA adjuvant by the intramuscular (i.m.) route at the same time of DNA immunization, as indicated.

[b] For the boosting immunizations, the individual V1V2 scaffold protein (100 μg/dose) formulated with IFA adjuvant was administered by the i.m. route.

[c] One animal (animal H3.5.4) had to be terminated early due to health issues.

two protein immunogens we had tested in the rabbit H2 experiment, V1V2(ZM53)-2J9C (H3.4) and V1V2(ZM109)-TTB (H3.5). The priming was then followed by two protein boosts with the same protein immunogens.

Sera from the animals for both H2 and H3 experiments displayed strong and distinct Ab responses to our immunogens as assessed by ELISA. To detect the Ab responses, we used three V1V2 antigen probes, including the structurally constrained V1V2(ZM109)-1FD6 (Fig. 3A) and V1V2(CAP45)-1FD6 (Fig. 3B), which had been used in complex with PG9 and PG16 for crystallization (33), as well as the unconstrained V1V2(1086)-tags (Fig. 3C) (23). All three antigens used in ELISAs carried V1V2 regions derived from clade C viruses, but their sequences differed. The Ab responses clearly separated into two distinct groups based on their ELISA binding to the structurally constrained probes (Fig. 3A and B) and the unconstrained probe (Fig. 3C). Thus, the structurally constrained V1V2 immunogens induced strong Ab responses reactive with the structurally constrained antigen probes V1V2(ZM109)-1FD6 and V1V2(CAP45)-1FD6, while the unconstrained immunogens, V1V2(1086)-Fc and V1V2(ZM109)-Fc, were the only immunogens that induced Abs recognized, albeit more weakly, by the unconstrained antigen V1V2(1086)-tags. Although Abs induced by gp120(ZM109) could recognize V1V2(ZM109)-1FD6, their binding was reduced against the heterologous V1V2(CAP45)-1FD6 probe, suggesting that gp120(ZM109) induced more sequence-specific Ab responses. Interestingly, in experiment H3, the structurally unconstrained V1V2(ZM109)-Fc was able to induce strong Ab responses against the constrained scaffolded V1V2 probes, which is substantially different from the results of the V1V2(1086)-Fc in experiment H2 (Fig. 3A and B). This result suggested that the amino acid sequence could influence the structural conformation in the construct. However, the epitope specificity of the Ab responses induced by the structurally unconstrained V1V2(ZM109)-Fc was different from that of the

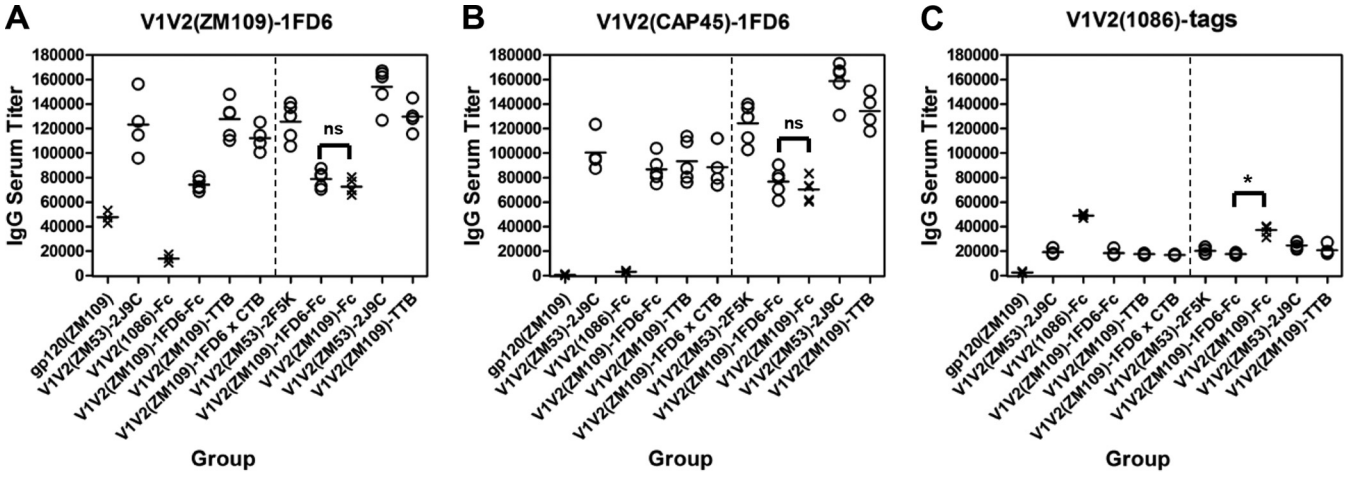

FIG 3 Endpoint titers of the rabbit Ab responses of the V1V2 immunogens. Endpoint binding titers of sera for all the H2 and H3 rabbits were measured by ELISA against the structurally constrained V1V2(ZM109)-1FD6 (A) and V1V2(CAP45)-1FD6 (B) and the unconstrained V1V2(1086)-tags (C). Each point represents the average titer calculated from duplicate samples of individual rabbits. The data points of sera from animals immunized with structurally unconstrained immunogens are marked by crosses while that with the constrained immunogens are marked by open circles. The vertical dashed line in each panel separates the H2 and H3 animal groups. The statistical difference between the Ab responses in H2 induced by the structurally constrained and unconstrained immunogens measured against V1V2(ZM109)-1FD6 and V1V2(CAP45)-1FD6 is highly significant ($P < 0.0001$). The statistical differences between the Ab responses induced by the structurally constrained V1V2(ZM109)-1FD6-Fc and the unconstrained V1V2(ZM109)-Fc are indicated. ns, not significant; *, $P < 0.05$.

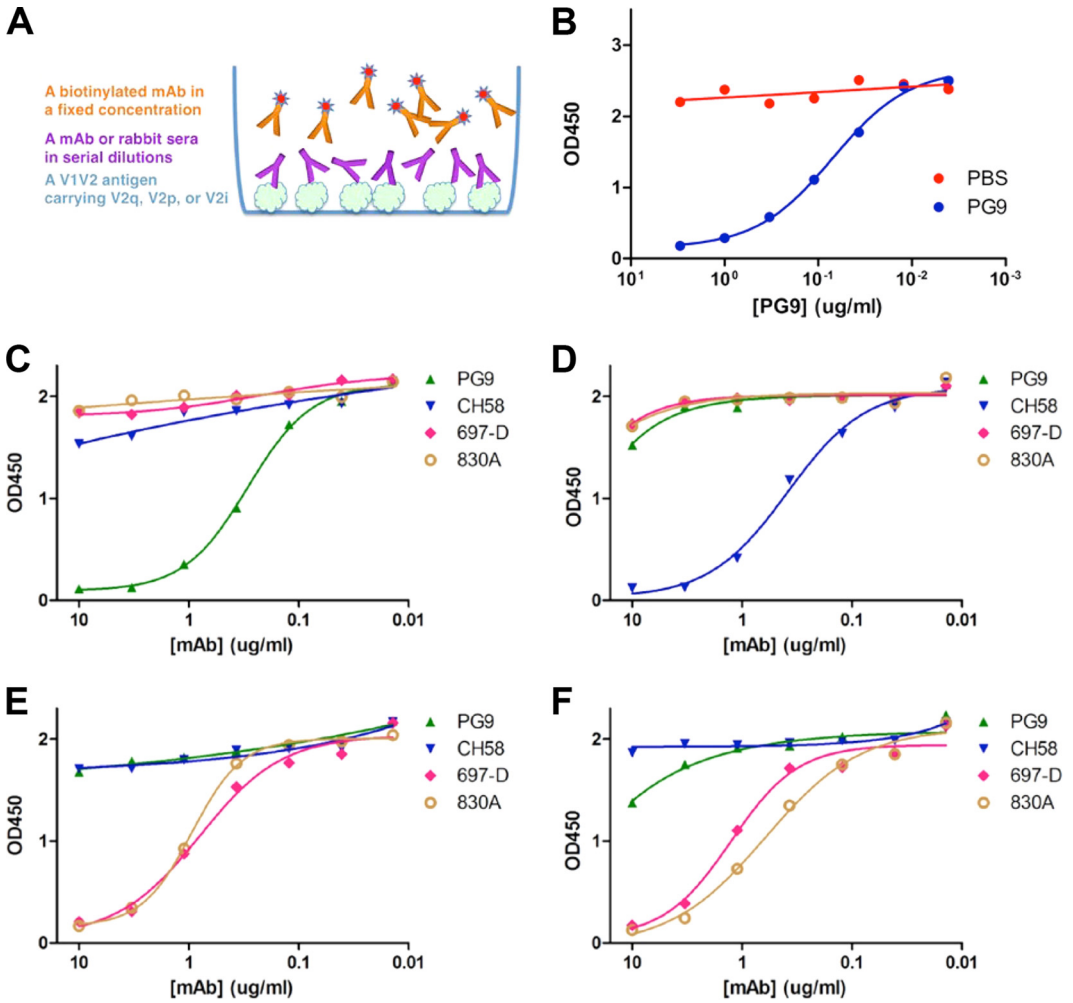

FIG 4 Competition of V1V2 MAbs against each other. (A) An illustration of the competition assay setup. (B) To establish the baseline, we first competed each V1V2 MAb against itself. Shown here is V2q MAb PG9 competed with itself for structurally constrained antigen V1V2(ZM109)-1FD6 coated on the plate using PBS as a negative control. (C to F) Competition of V2q MAb PG9, V2i MAbs 697-D and 830A, and V2p MAb CH58 by biotinylated MAbs PG9 (C), 697-D (E), and 830A (F) for V1V2(ZM109)-1FD6 coated on the plates. Panel D shows competition of the same MAbs by biotinylated V2p MAb CH58 for V1V2(1086)-tags. Note that PG9 and CH58 each only competed with itself (C and D), while V2i MAb 830A and 697-D competed with each other. Although CH58 does not bind V1V2(ZM109)-1FD6 and PG9 does not bind V1V2(1086)-tags, they were included for references.

constrained V1V2(ZM109)-1FD6-Fc, as revealed by the competition assay (see below).

V1V2-scaffold immunogens induce distinct conformation-specific V1V2-directed Ab responses. To gain additional understanding of the conformational specificities of the Ab responses induced by V1V2-scaffold immunogens in rabbits, we performed an Ab competition assay for the rabbit immune sera with the V2q MAb PG9, V2p MAb CH58, and V2i MAbs 697-D and 830A (Fig. 4 and 5). In this assay, we coated the plates with antigen probes that carry different epitope types and competed the rabbit sera with biotinylated MAbs. These V1V2 MAbs were used first to compete against each other (Fig. 4). The data showed that only the two V2i MAbs, 697-D and 830A, competed against each other, further illustrating the distinctness of the three types of V1V2 epitopes. Rabbit sera taken 2 weeks after the last protein boost were then used to compete against V1V2 MAbs (Fig. 5). Serum from individual rabbits of each group was tested separately, and only the curve of a representative rabbit of the groups that demonstrated clear competition is shown in Fig. 5. Sera from rabbit groups immunized by the structurally constrained immunogens V1V2(ZM53)-2J9C (Fig. 5A, represented by rabbit numbers H2.2.1 and H3.4.1), V1V2(ZM109)-TTB (Fig. 5A, H2.5.1), and V1V2(ZM109)-1FD6-Fc (Fig. 5A, H2.4.1) showed pronounced competition against PG9 for the binding of V1V2(ZM109)-1FD6, suggesting that these immunogens induced Abs whose epitopes overlap, and are conformationally similar to, the V2q epitopes. There was variation between animals: serum from rabbit H2.4.3 did not show strong competition with PG9, unlike that of rabbit H2.4.1, as shown in Fig. 5, and of the other three rabbits in the group. On the other hand, sera from rabbits of the group immunized with V1V2(1086)-Fc (H2.3.2) competed well with the V2p MAb CH58 for binding to V1V2(1086)-tags. Interestingly, sera from rabbits immunized with the trimeric immunogens V1V2(M53)-2J9C (Fig. 5B, H2.2.1 and H3.4.1) and V1V2(M53)-2F5K (Fig. 5B, H3.1.1) could also compete with CH58 with modest strength, suggesting that these constructs can also sample the helical confor-

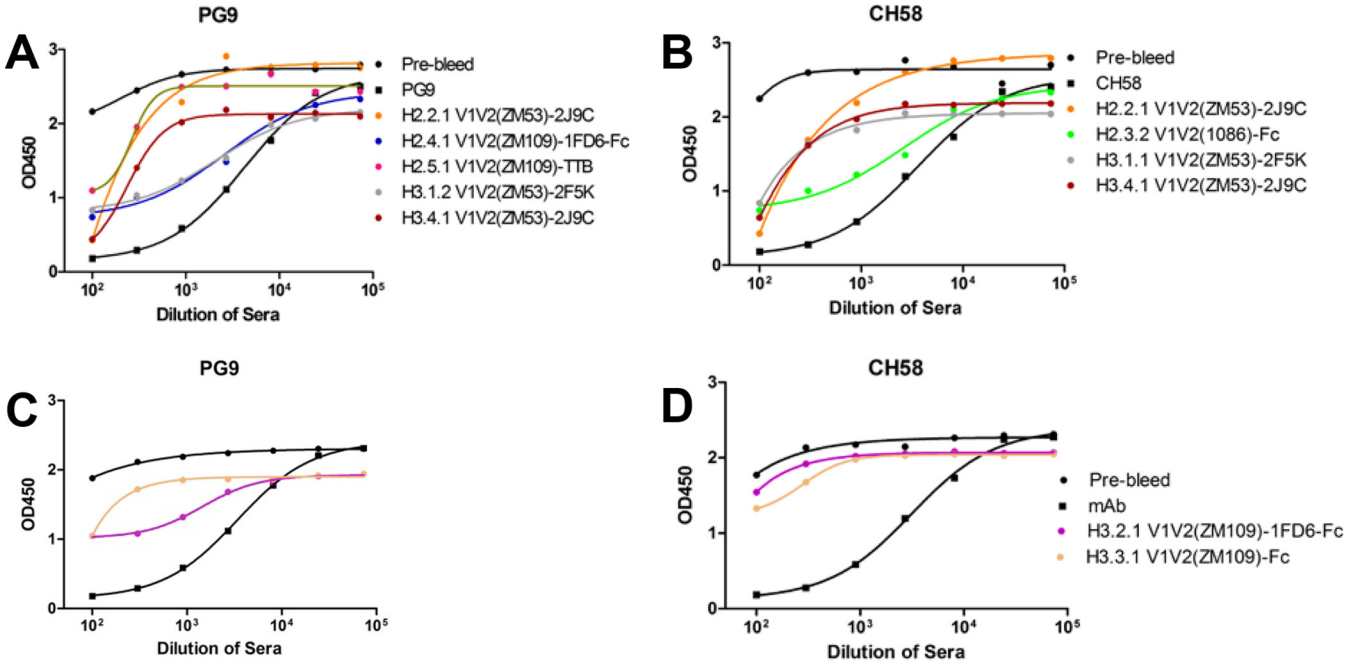

FIG 5 Competition of rabbit sera against V1V2 MAbs. (A and B) Results of rabbit sera competed against V2q MAb PG9 and V2p MAb CH58. As references, black curves from data of prebleeds and competition against the same MAb are included. (C and D) Competition against V2q MAb PG9 and V2p MAb CH58, as indicated, by sera from rabbits immunized with either structurally constrained V1V2(ZM109)-1FD6-Fc or the unconstrained V1V2(ZM109)-Fc.

mations. In contrast, no serum gave very strong competition against the V2i MAbs 697-D and 830A (data not shown). Figures 5C and D illustrate the difference in the Abs induced by the two immunogens V1V2(ZM109)-1FD6-Fc and V1V2(ZM109)-Fc that have the same V1V2 sequence. The structurally constrained V1V2(ZM109)-1FD6-Fc clearly induced Abs that could compete strongly with PG9, while the Abs induced by the unconstrained V1V2(ZM109)-Fc could compete very little (Fig. 5C). Interestingly V1V2(ZM109)-Fc (Fig. 5D) did not induce Abs that could compete strongly with CH58, unlike Abs induced by V1V2 (1086)-Fc (Fig. 5B, H2.3.2).

V1V2 immunogen-induced antibody neutralization. We assessed the neutralizing activity of all immune sera from experiment H3 using the TZM.bl assay under conditions in which the virus and sera were incubated together for either 30 min or 24 h prior to addition to cells, as per previous studies (53); the pseudoviruses of strains MW965 and ZM109 were used (Table 4 and Fig. 6, respectively). Although strains MW965 (tier 1A) and ZM109 (tier 1B) are neutralization-sensitive viruses, they could not be neutralized by the RV144 V2p MAb CH58 (data not shown). Sera drawn 2 weeks after the last boost from almost all animals achieved neutralization of MW965 in the 30-min assay while all sera achieved 50% neutralization in the 24-h assay (Table 4). In assays using the tier 1B strain ZM109 (Fig. 6) in the 24-h assay, sera from four of the five groups in experiment H3, boosted with the structurally constrained V1V2(ZM109)-1FD6-Fc or V1V2(ZM53)-2J9C, gave ≥50% neutralization (values above the dashed line in Fig. 6B). Since the V1V2 sequence of V1V2(ZM53)-2J9C used in immunizing group H3.4 is different from that of ZM109, the immune sera of this group achieved heterologous neutralization in the 24-h assay. Sera from two animals immunized with another trimeric protein, V1V2(ZM53)-2F5K, also achieved heterologous neutralization of ZM109 in the 24-h assay.

DISCUSSION

Data from the RV144 phase III vaccine trial, the only HIV/AIDS vaccine trial that demonstrated modest 31.2% efficacy, suggested that the V1V2 region of HIV-1 gp120 is a key vaccine target (31, 35–37). Clearly, a more efficacious vaccine is needed. Based on data of MAbs isolated from an RV144 vaccinee, we know that V2p Abs were induced (23). However, the absence of strong neutralizing activity in RV144 sera suggests that V2q Abs were not induced (38). Which, if any, of these types of V2 Abs were directly responsible for the reduced rate of infection is not known at this point. However, our classification of V1V2 epitopes into three distinct types, i.e., the V2q, V2p, and V2i types, provided a conceptual starting point for designing immunogens that can focus the immune responses to each of these types (26, 27).

Structural studies of V1V2 and the MAbs that bind to the V2p/V2q epitope region have illuminated the structural complexity of this region, indicating that it can assume at least two conformations: one that is recognized by V2p MAbs in which the strand C region assumes a helical conformation appeared to be present in molecules in which V1V2 is not constrained, such as V1V2(1086)-tags (Fig. 2C) (23), and one that is recognized by V2q MAbs in which the region is present as a β-strand, as in the case of molecules where V1V2 is constrained, such as V1V2(ZM109)-1FD6 and V1V2(CAP45)-1FD6 (33, 34). However, the V2i epitopes do not overlap V2p and V2q epitopes (Fig. 4) (6), and V2i Abs can recognize V1V2 constructs harboring both conformations (Table 2).

We have shown here that we could design immunogens targeting the helical V2p and β-stranded V2q epitope types. In particular, the structurally constrained V1V2-scaffold proteins, such as the trimeric V1V2(ZM53)-2J9C and V1V2(ZM53)-2F5K and the pentameric V1V2(ZM109)-TTB, can harbor the β-stranded conformation

TABLE 4 The inhibitory dose titers of the H3 rabbit sera against MW965 in a 30-min and a 24-h TZM.bl neutralization assay[a]

Serum #	Rabbit #	MW965 (clade C)					
		30 min			24h		
		ID50	ID80	ID90	ID50	ID80	ID90
1	H3.1.1	264	60	<10	1766	806	663
2	H3.1.2	40	15	<10	1633	459	316
3	H3.1.3	10	<10	<10	108	19	13
4	H3.1.4	56	22	<10	2575	613	287
5	H3.1.5	61	40	35	3907	1454	803
6	H3.2.1	29	<10	<10	1006	298	187
7	H3.2.2	14	<10	<10	668	98	61
8	H3.2.3	11	<10	<10	1020	62	30
9	H3.2.4	12	<10	<10	1119	167	78
10	H3.2.5	<10	<10	<10	24	16	13
11	H3.3.1	12	10	<10	377	81	55
12	H3.3.2	36	25	<10	1378	272	151
13	H3.3.3	13	<10	<10	513	141	101
14	H3.3.4	12	<10	<10	191	62	37
15	H3.3.5	16	<10	<10	792	190	132
16	H3.4.1	<10	<10	<10	136	65	41
17	H3.4.2	11	<10	<10	357	160	102
18	H3.4.3	39	<10	<10	845	287	159
19	H3.4.4	11	<10	<10	251	119	79
20	H3.4.5	10	<10	<10	216	107	73
21	H3.5.1	11	<10	<10	354	134	104
22	H3.5.2	12	<10	<10	392	98	64
23	H3.5.3	17	<10	<10	417	115	75
25	H3.5.5	25	14	10	1064	426	295

[a] ID50, ID80, and ID90 are the 50%, 80%, and 90% inhibitory doses, respectively.

while the simple Fc fusion forms of V1V2 carry the helical conformation of the epitopes. These epitope scaffold immunogens can induce distinct Ab responses in rabbits, i.e., the unconstrained immunogens induced Abs that reacted preferentially with the unconstrained antigen V1V2(1086)-tags, while the constrained immunogens induced Abs that reacted preferentially with the constrained antigens V1V2(ZM109)-1FD6 and V1V2(CAP45)-1FD6 (Fig. 3). Moreover, the Abs induced by the immunogens carrying the V2q epitopes could compete with the V2q MAbs PG9 while those induced by the immunogens carrying the V2p epitopes could compete with the V2p MAbs CH58 (Fig. 5). In addition, sera of several rabbits could neutralize the tier 1A virus MW965, which is heterologous to the immunizing strains, and the tier 1B virus ZM109 in the 24-h incubation assay (Table 4 and Fig. 6), representing a significant improvement from the V1V2 Abs induced by the RV144 vaccines.

These rabbit experiments are among the first to demonstrate that the immune response can be focused on the V1V2 region (54). The cross-reactivity of human V1V2 Abs has long been established although this region has the most sequence and length diversity in the HIV-1 Env (22). This immunologic cross-reactivity in the face of variable amino acid sequences as well as insertions and deletions can be explained on the basis of the structural data that have emerged in the last few years. Thus, the β-barrel structure that has been described for V1V2 likely forms a conserved functional module (6), which not only explains the conserved antigenic structure that allows antigenic cross-reactivity but also allows the transplantation of the whole domain into scaffolds by rational structural designs.

The Ab response to V1V2 in HIV-infected individuals is less robust than that to V3 or the CD4-binding site (22, 55, 56), and V1V2 Ab responses were of a much smaller magnitude in previous vaccine studies than in the RV144 study, suggesting that despite its prominent location on the Env spike, V1V2 is not an immunodominant epitope region. We have shown in the data presented here that presenting V1V2 in a multivalent scaffold overcomes its relatively poor immunogenicity as well as inducing cross-reactive Abs. To induce even higher levels of Abs, these constructs can be readily modified to form nanoparticles, such as virus-like particles, which will present the V1V2 domain at even higher valences capable of improved interaction with B cell receptors. These studies are currently ongoing.

Our data further demonstrate that one can selectively focus the Ab response on particular conformations of an epitope region. The helical conformation of the V2p epitope is likely a means of masking the vulnerable β-strand conformation of the same region. Side chains of a helix point away from the helix axis, and helix-specific Abs are generally side chain specific. From the point of view of the virus, helix-specific Abs would be preferential since virus escape by mutation from such Abs would be relatively simple. Escape from complex conformational epitopes, such as those targeted by V2q and V2i Abs, would be more complicated. The distinct characteristics of the Abs induced by structurally constrained immunogens and those induced by the unconstrained ones (Fig. 3 and 5) suggest that the rabbit immune system responded differently against the two types of immunogens.

Data presented here suggest that our immunogens could serve as prototype vaccine candidates targeting the V1V2. While novel in the current iterations, improvements could induce Abs that are more V2q-like. For example, trimer-specific MAbs like PGT145 were shown to bind close to the axis of the Env trimer, and their epitopes are likely V1V2 specific (57); but our two trimeric immunogens were not recognized by PGT145 (data not shown). Since our trimeric scaffolds are recognized by PG9, the C strand of the V1V2 apex is likely correctly formed; thus, their orientation toward the trimer axis may deviate from that of the epitope of PGT145. Such orientation can be adjusted at the V1V2-scaffold junction, and computational modeling in combination with antigenicity testing will be able to identify improved constructs. Furthermore, the current V1V2 constructs, even the structurally constrained ones, are likely to be able to sample different conformations so that the trimeric immunogens could induce Abs that compete with the V2p MAb CH58. Additional stabilizations may reduce such dynamic sampling between conformations. Finally, the different functional activities of V1V2(ZM109)-Fc and V1V2(1086)-Fc suggested that the amino acid sequence of

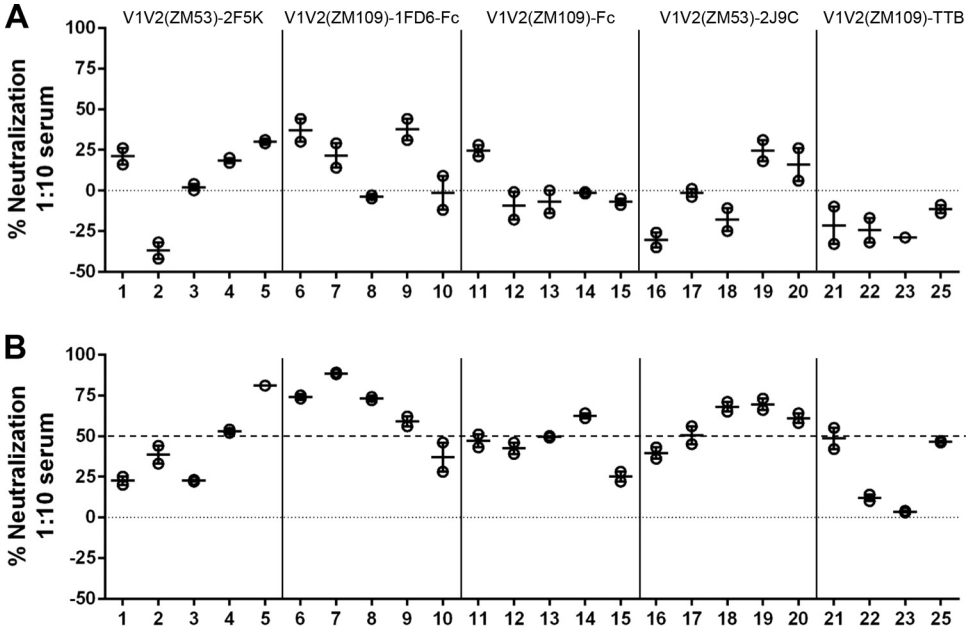

FIG 6 Neutralization assays. Neutralization of the H3 rabbit sera was determined against the tier 1B ZM109 strain in 30-min (A) and 24-h (B) incubation neutralization assays. Vertical lines separate each animal group, and the boosting immunogen used for each group is labeled at the top of the two panels. The assays were duplicated, and the horizontal lines in the data points indicate the averages. Note that sera of several animals, including those immunized with trimeric immunogens V1V2(ZM53)-2F5K and V1V2(ZM53)-2J9C, which have a V1V2 sequence heterologous from that of ZM109, reached above 50% neutralization (dashed line) in the 24-h incubation.

V1V2 can also play a role in their function. Therefore, sequence selection is another area for potential improvement, with attention paid to both amino acid sequence and variable loop lengths (58). We anticipate that a combination of sequence selection, structure-based design, and formulation as highly multivalent constructs will likely lead to V1V2 immunogens with superior ability to focus the Ab response on this site of vulnerability and with increased immunogenicity.

ACKNOWLEDGMENT

We thank Gary Nabel for the pVRC8400 plasmid and Peter Kwong for the original constructs of V1V2(ZM109)-1FD6 and V1V2(CAP45)-1FD6.

This work was supported in part by the National Institutes of Health under award number P01 AI100151 and by funds from Icahn School of Medicine at Mount Sinai.

The content is solely the responsibility of the authors and does not necessarily represent the official views of the National Institutes of Health.

FUNDING INFORMATION

This work, including the efforts of Xunqing Jiang, Max Totrov, Wei Li, Jared M. Sampson, Constance Williams, Shan Lu, Shixia Wang, Susan Zolla-Pazner, and Xiang-Peng Kong, was funded by HHS | NIH | National Institute of Allergy and Infectious Diseases (NIAID) (P01AI100151). This work, including the efforts of Hong Lu and Xueling Wu, was funded by HHS | NIH | National Institute of Allergy and Infectious Diseases (NIAID) (R01AI114380).

REFERENCES

1. **Wyatt R, Sodroski J.** 1998. The HIV-1 envelope glycoproteins: fusogens, antigens, and immunogens. Science **280:**1884–1888. http://dx.doi.org/10.1126/science.280.5371.1884.
2. **Ward AB, Wilson IA.** 2015. Insights into the trimeric HIV-1 envelope glycoprotein structure. Trends Biochem Sci **40:**101–107. http://dx.doi.org/10.1016/j.tibs.2014.12.006.
3. **Modrow S, Hahn BH, Shaw GM, Gallo RC, Wong-Staal F, Wolf H.** 1987. Computer-assisted analysis of envelope protein sequences of seven human immunodeficiency virus isolates: prediction of antigenic epitopes in conserved and variable regions. J Virol **61:**570–578.
4. **Zolla-Pazner S, Cardozo T.** 2010. Structure-function relationships of HIV-1 envelope sequence-variable regions refocus vaccine design. Nat Rev Immunol **10:**527–535. http://dx.doi.org/10.1038/nri2801.
5. **Pancera M, Zhou T, Druz A, Georgiev IS, Soto C, Gorman J, Huang J, Acharya P, Chuang GY, Ofek G, Stewart-Jones GB, Stuckey J, Bailer RT, Joyce MG, Louder MK, Tumba N, Yang Y, Zhang B, Cohen MS, Haynes BF, Mascola JR, Morris L, Munro JB, Blanchard SC, Mothes W, Connors M, Kwong PD.** 2014. Structure and immune recognition of trimeric pre-fusion HIV-1 Env. Nature **514:**455–461. http://dx.doi.org/10.1038/nature13808.
6. **Pan R, Gorny MK, Zolla-Pazner S, Kong XP.** 2015. The V1V2 region of HIV-1 gp120 forms a five-stranded beta barrel. J Virol **89:**8003–8010. http://dx.doi.org/10.1128/JVI.00754-15.
7. **Julien JP, Cupo A, Sok D, Stanfield RL, Lyumkis D, Deller MC, Klasse PJ, Burton DR, Sanders RW, Moore JP, Ward AB, Wilson IA.** 2013. Crystal structure of a soluble cleaved HIV-1 envelope trimer. Science **342:**1477–1483. http://dx.doi.org/10.1126/science.1245625.
8. **Lyumkis D, Julien JP, de Val N, Cupo A, Potter CS, Klasse PJ, Burton DR, Sanders RW, Moore JP, Carragher B, Wilson IA, Ward AB.** 2013. Cryo-EM structure of a fully glycosylated soluble cleaved HIV-1 envelope trimer. Science **342:**1484–1490. http://dx.doi.org/10.1126/science.1245627.
9. **Lee JH, Ozorowski G, Ward AB.** 2016. Cryo-EM structure of a native, fully glycosylated, cleaved HIV-1 envelope trimer. Science **351:**1043–1048. http://dx.doi.org/10.1126/science.aad2450.
10. **Munro JB, Gorman J, Ma X, Zhou Z, Arthos J, Burton DR, Koff WC, Courter JR, Smith AB, III, Kwong PD, Blanchard SC, Mothes W.** 2014. Conformational dynamics of single HIV-1 envelope trimers on the surface of native virions. Science **346:**759–763. http://dx.doi.org/10.1126/science.1254426.
11. **Spurrier B, Sampson JM, Totrov M, Li H, O'Neal T, Williams C, Robinson J, Gorny MK, Zolla-Pazner S, Kong XP.** 2011. Structural analysis of human and macaque mAbs 2909 and 2.5B: implications for the configuration of the quaternary neutralizing epitope of HIV-1 gp120. Structure **19:**691–699. http://dx.doi.org/10.1016/j.str.2011.02.012.
12. **Arthos J, Cicala C, Martinelli E, Macleod K, Van Ryk D, Wei D, Xiao Z, Veenstra TD, Conrad TP, Lempicki RA, McLaughlin S, Pascuccio M,**

Gopaul R, McNally J, Cruz CC, Censoplano N, Chung E, Reitano KN, Kottilil S, Goode DJ, Fauci AS. 2008. HIV-1 envelope protein binds to and signals through integrin $\alpha_4\beta_7$, the gut mucosal homing receptor for peripheral T cells. Nat Immunol **9:**301–309. http://dx.doi.org/10.1038/ni1566.

13. **Tassaneetrithep B, Tivon D, Swetnam J, Karasavvas N, Michael NL, Kim JH, Marovich M, Cardozo T.** 2014. Cryptic determinant of α4β7 binding in the V2 loop of HIV-1 gp120. PLoS One **9:**e108446. http://dx.doi.org/10.1371/journal.pone.0108446.
14. **Peachman KK, Karasavvas N, Chenine AL, McLinden R, Rerks-Ngarm S, Jaranit K, Nitayaphan S, Pitisuttithum P, Tovanabutra S, Zolla-Pazner S, Michael NL, Kim JH, Alving CR, Rao M.** 2015. Identification of new regions in HIV-1 gp120 variable 2 and 3 loops that bind to α4β7 integrin receptor. PLoS One **10:**e0143895. http://dx.doi.org/10.1371/journal.pone.0143895.
15. **Ratner L, Fisher A, Jagodzinski LL, Mitsuya H, Liou RS, Gallo RC, Wong-Staal F.** 1987. Complete nucleotide sequences of functional clones of the AIDS virus. AIDS Res Hum Retroviruses **3:**57–69. http://dx.doi.org/10.1089/aid.1987.3.57.
16. **Moore JP, Sattentau QJ, Yoshiyama H, Thali M, Charles M, Sullivan N, Poon SW, Fung MS, Traincard F, Pinkus M, Robey G, Robinson JE, Ho DD, Sodroski J.** 1993. Probing the structure of the V2 domain of human immunodeficiency virus type 1 surface glycoprotein gp120 with a panel of eight monoclonal antibodies: human immune response to the V1 and V2 domains. J Virol **67:**6136–6151.
17. **Gorny MK, Moore JP, Conley AJ, Karwowska S, Sodroski J, Williams C, Burda S, Boots LJ, Zolla-Pazner S.** 1994. Human anti-V2 monoclonal antibody that neutralizes primary but not laboratory isolates of human immunodeficiency virus type 1. J Virol **68:**8312–8320.
18. **Gorny MK, Stamatatos L, Volsky B, Revesz K, Williams C, Wang XH, Cohen S, Staudinger R, Zolla-Pazner S.** 2005. Identification of a new quaternary neutralizing epitope on human immunodeficiency virus type 1 virus particles. J Virol **79:**5232–5237. http://dx.doi.org/10.1128/JVI.79.8.5232-5237.2005.
19. **Walker LM, Phogat SK, Chan-Hui PY, Wagner D, Phung P, Goss JL, Wrin T, Simek MD, Fling S, Mitcham JL, Lehrman JK, Priddy FH, Olsen OA, Frey SM, Hammond PW, Kaminsky S, Zamb T, Moyle M, Koff WC, Poignard P, Burton DR.** 2009. Broad and potent neutralizing antibodies from an African donor reveal a new HIV-1 vaccine target. Science **326:**285–289. http://dx.doi.org/10.1126/science.1178746.
20. **Bonsignori M, Hwang KK, Chen X, Tsao CY, Morris L, Gray E, Marshall DJ, Crump JA, Kapiga SH, Sam NE, Sinangil F, Pancera M, Yongping Y, Zhang B, Zhu J, Kwong PD, O'Dell S, Mascola JR, Wu L, Nabel GJ, Phogat S, Seaman MS, Whitesides JF, Moody MA, Kelsoe G, Yang X, Sodroski J, Shaw GM, Montefiori DC, Kepler TB, Tomaras GD, Alam SM, Liao HX, Haynes BF.** 2011. Analysis of a clonal lineage of HIV-1 envelope V2/V3 conformational epitope-specific broadly neutralizing antibodies and their inferred unmutated common ancestors. J Virol **85:**9998–10009. http://dx.doi.org/10.1128/JVI.05045-11.
21. **Doria-Rose NA, Schramm CA, Gorman J, Moore PL, Bhiman JN, DeKosky BJ, Ernandes MJ, Georgiev IS, Kim HJ, Pancera M, Staupe RP, Altae-Tran HR, Bailer RT, Crooks ET, Cupo A, Druz A, Garrett NJ, Hoi KH, Kong R, Louder MK, Longo NS, McKee K, Nonyane M, O'Dell S, Roark RS, Rudicell RS, Schmidt SD, Sheward DJ, Soto C, Wibmer CK, Yang Y, Zhang Z, Program NCS, Mullikin JC, Binley JM, Sanders RW, Wilson IA, Moore JP, Ward AB, Georgiou G, Williamson C, Abdool Karim SS, Morris L, Kwong PD, Shapiro L, Mascola JR.** 2014. Developmental pathway for potent V1V2-directed HIV-neutralizing antibodies. Nature **509:**55–62. http://dx.doi.org/10.1038/nature13036.
22. **Israel ZR, Gorny MK, Palmer C, McKeating JA, Zolla-Pazner S.** 1997. Prevalence of a V2 epitope in clade B primary isolates and its recognition by sera from HIV-1-infected individuals. AIDS **11:**128–130.
23. **Liao HX, Bonsignori M, Alam SM, McLellan JS, Tomaras GD, Moody MA, Kozink DM, Hwang KK, Chen X, Tsao CY, Liu P, Lu X, Parks RJ, Montefiori DC, Ferrari G, Pollara J, Rao M, Peachman KK, Santra S, Letvin NL, Karasavvas N, Yang ZY, Dai K, Pancera M, Gorman J, Wiehe K, Nicely NI, Rerks-Ngarm S, Nitayaphan S, Kaewkungwal J, Pitisuttithum P, Tartaglia J, Sinangil F, Kim JH, Michael NL, Kepler TB, Kwong PD, Mascola JR, Nabel GJ, Pinter A, Zolla-Pazner S, Haynes BF.** 2013. Vaccine induction of antibodies against a structurally heterogeneous site of immune pressure within HIV-1 envelope protein variable regions 1 and 2. Immunity **38:**176–186. http://dx.doi.org/10.1016/j.immuni.2012.11.011.
24. **Corti D, Langedijk JP, Hinz A, Seaman MS, Vanzetta F, Fernandez-Rodriguez BM, Silacci C, Pinna D, Jarrossay D, Balla-Jhagjhoorsingh S, Willems B, Zekveld MJ, Dreja H, O'Sullivan E, Pade C, Orkin C, Jeffs SA, Montefiori DC, Davis D, Weissenhorn W, McKnight A, Heeney JL, Sallusto F, Sattentau QJ, Weiss RA, Lanzavecchia A.** 2010. Analysis of memory B cell responses and isolation of novel monoclonal antibodies with neutralizing breadth from HIV-1-infected individuals. PLoS One **5:**e8805. http://dx.doi.org/10.1371/journal.pone.0008805.
25. **Scheid JF, Mouquet H, Feldhahn N, Seaman MS, Velinzon K, Pietzsch J, Ott RG, Anthony RM, Zebroski H, Hurley A, Phogat A, Chakrabarti B, Li Y, Connors M, Pereyra F, Walker BD, Wardemann H, Ho D, Wyatt RT, Mascola JR, Ravetch JV, Nussenzweig MC.** 2009. Broad diversity of neutralizing antibodies isolated from memory B cells in HIV-infected individuals. Nature **458:**636–640. http://dx.doi.org/10.1038/nature07930.
26. **Mayr LM, Cohen S, Spurrier B, Kong XP, Zolla-Pazner S.** 2013. Epitope mapping of conformational V2-specific anti-HIV human monoclonal antibodies reveals an immunodominant site in V2. PLoS One **8:**e70859. http://dx.doi.org/10.1371/journal.pone.0070859.
27. **Spurrier B, Sampson J, Gorny MK, Zolla-Pazner S, Kong XP.** 2014. Functional implications of the binding mode of a human conformation-dependent V2 monoclonal antibody against HIV. J Virol **88:**4100–4112. http://dx.doi.org/10.1128/JVI.03153-13.
28. **Gorny MK, Pan R, Williams C, Wang XH, Volsky B, O'Neal T, Spurrier B, Sampson JM, Li L, Seaman MS, Kong XP, Zolla-Pazner S.** 2012. Functional and immunochemical cross-reactivity of V2-specific monoclonal antibodies from HIV-1-infected individuals. Virology **427:**198–207. http://dx.doi.org/10.1016/j.virol.2012.02.003.
29. **Nyambi PN, Mbah HA, Burda S, Williams C, Gorny MK, Nadas A, Zolla-Pazner S.** 2000. Conserved and exposed epitopes on intact, native, primary human immunodeficiency virus type 1 virions of group M. J Virol **74:**7096–7107. http://dx.doi.org/10.1128/JVI.74.15.7096-7107.2000.
30. **Pinter A, Honnen WJ, He Y, Gorny MK, Zolla-Pazner S, Kayman SC.** 2004. The V1/V2 domain of gp120 is a global regulator of the sensitivity of primary human immunodeficiency virus type 1 isolates to neutralization by antibodies commonly induced upon infection. J Virol **78:**5205–5215. http://dx.doi.org/10.1128/JVI.78.10.5205-5215.2004.
31. **Rerks-Ngarm S, Pitisuttithum P, Nitayaphan S, Kaewkungwal J, Chiu J, Paris R, Premsri N, Namwat C, de Souza M, Adams E, Benenson M, Gurunathan S, Tartaglia J, McNeil JG, Francis DP, Stablein D, Birx DL, Chunsuttiwat S, Khamboonruang C, Thongcharoen P, Robb ML, Michael NL, Kunasol P, Kim JH.** 2009. Vaccination with ALVAC and AIDSVAX to prevent HIV-1 infection in Thailand. N Engl J Med **361:**2209–2220. http://dx.doi.org/10.1056/NEJMoa0908492.
32. **Bonsignori M, Pollara J, Moody MA, Alpert MD, Chen X, Hwang KK, Gilbert PB, Huang Y, Gurley TC, Kozink DM, Marshall DJ, Whitesides JF, Tsao CY, Kaewkungwal J, Nitayaphan S, Pitisuttithum P, Rerks-Ngarm S, Kim JH, Michael NL, Tomaras GD, Montefiori DC, Lewis GK, DeVico A, Evans DT, Ferrari G, Liao HX, Haynes BF.** 2012. Antibody-dependent cellular cytotoxicity-mediating antibodies from an HIV-1 vaccine efficacy trial target multiple epitopes and preferentially use the VH1 gene family. J Virol **86:**11521–11532. http://dx.doi.org/10.1128/JVI.01023-12.
33. **McLellan JS, Pancera M, Carrico C, Gorman J, Julien JP, Khayat R, Louder R, Pejchal R, Sastry M, Dai K, O'Dell S, Patel N, Shahzad-ul Hussan S, Yang Y, Zhang B, Zhou T, Zhu J, Boyington JC, Chuang GY, Diwanji D, Georgiev I, Kwon YD, Lee D, Louder MK, Moquin S, Schmidt SD, Yang ZY, Bonsignori M, Crump JA, Kapiga SH, Sam NE, Haynes BF, Burton DR, Koff WC, Walker LM, Phogat S, Wyatt R, Orwenyo J, Wang LX, Arthos J, Bewley CA, Mascola JR, Nabel GJ, Schief WR, Ward AB, Wilson IA, Kwong PD.** 2011. Structure of HIV-1 gp120 V1/V2 domain with broadly neutralizing antibody PG9. Nature **480:**336–343. http://dx.doi.org/10.1038/nature10696.
34. **Pancera M, Shahzad-Ul-Hussan S, Doria-Rose NA, McLellan JS, Bailer RT, Dai K, Loesgen S, Louder MK, Staupe RP, Yang Y, Zhang B, Parks R, Eudailey J, Lloyd KE, Blinn J, Alam SM, Haynes BF, Amin MN, Wang LX, Burton DR, Koff WC, Nabel GJ, Mascola JR, Bewley CA, Kwong PD.** 2013. Structural basis for diverse N-glycan recognition by HIV-1-neutralizing V1-V2-directed antibody PG16. Nat Struct Mol Biol **20:**804–813. http://dx.doi.org/10.1038/nsmb.2600.
35. **Haynes BF, Gilbert PB, McElrath MJ, Zolla-Pazner S, Tomaras GD, Alam SM, Evans DT, Montefiori DC, Karnasuta C, Sutthent R, Liao HX, DeVico AL, Lewis GK, Williams C, Pinter A, Fong Y, Janes H,**

DeCamp A, Huang Y, Rao M, Billings E, Karasavvas N, Robb ML, Ngauy V, de Souza MS, Paris R, Ferrari G, Bailer RT, Soderberg KA, Andrews C, Berman PW, Frahm N, De Rosa SC, Alpert MD, Yates NL, Shen X, Koup RA, Pitisuttithum P, Kaewkungwal J, Nitayaphan S, Rerks-Ngarm S, Michael NL, Kim JH. 2012. Immune-correlates analysis of an HIV-1 vaccine efficacy trial. N Engl J Med **366:**1275–1286. http://dx.doi.org/10.1056/NEJMoa1113425.

36. **Zolla-Pazner S, deCamp A, Gilbert PB, Williams C, Yates NL, Williams WT, Howington R, Fong Y, Morris DE, Soderberg KA, Irene C, Reichman C, Pinter A, Parks R, Pitisuttithum P, Kaewkungwal J, Rerks-Ngarm S, Nitayaphan S, Andrews C, O'Connell RJ, Yang ZY, Nabel GJ, Kim JH, Michael NL, Montefiori DC, Liao HX, Haynes BF, Tomaras GD.** 2014. Vaccine-induced IgG antibodies to V1V2 regions of multiple HIV-1 subtypes correlate with decreased risk of HIV-1 infection. PLoS One **9:**e87572. http://dx.doi.org/10.1371/journal.pone.0087572.
37. **Zolla-Pazner S, deCamp AC, Cardozo T, Karasavvas N, Gottardo R, Williams C, Morris DE, Tomaras G, Rao M, Billings E, Berman P, Shen X, Andrews C, O'Connell RJ, Ngauy V, Nitayaphan S, de Souza M, Korber B, Koup R, Bailer RT, Mascola JR, Pinter A, Montefiori D, Haynes BF, Robb ML, Rerks-Ngarm S, Michael NL, Gilbert PB, Kim JH.** 2013. Analysis of V2 antibody responses induced in vaccinees in the ALVAC/AIDSVAX HIV-1 vaccine efficacy trial. PLoS One **8:**e53629. http://dx.doi.org/10.1371/journal.pone.0053629.
38. **Montefiori DC, Karnasuta C, Huang Y, Ahmed H, Gilbert P, de Souza MS, McLinden R, Tovanabutra S, Laurence-Chenine A, Sanders-Buell E, Moody MA, Bonsignori M, Ochsenbauer C, Kappes J, Tang H, Greene K, Gao H, LaBranche CC, Andrews C, Polonis VR, Rerks-Ngarm S, Pitisuttithum P, Nitayaphan S, Kaewkungwal J, Self SG, Berman PW, Francis D, Sinangil F, Lee C, Tartaglia J, Robb ML, Haynes BF, Michael NL, Kim JH.** 2012. Magnitude and breadth of the neutralizing antibody response in the RV144 and Vax003 HIV-1 vaccine efficacy trials. J Infect Dis **206:**431–441. http://dx.doi.org/10.1093/infdis/jis367.
39. **Rolland M, Edlefsen PT, Larsen BB, Tovanabutra S, Sanders-Buell E, Hertz T, deCamp AC, Carrico C, Menis S, Magaret CA, Ahmed H, Juraska M, Chen L, Konopa P, Nariya S, Stoddard JN, Wong K, Zhao H, Deng W, Maust BS, Bose M, Howell S, Bates A, Lazzaro M, O'Sullivan A, Lei E, Bradfield A, Ibitamuno G, Assawadarachai V, O'Connell RJ, deSouza MS, Nitayaphan S, Rerks-Ngarm S, Robb ML, McLellan JS, Georgiev I, Kwong PD, Carlson JM, Michael NL, Schief WR, Gilbert PB, Mullins JI, Kim JH.** 2012. Increased HIV-1 vaccine efficacy against viruses with genetic signatures in Env V2. Nature **490:**417–420. http://dx.doi.org/10.1038/nature11519.
40. **Abagyan R, Totrov M, Kuznetsov D.** 1994. ICM—a new method for protein modeling and design: applications to docking and structure prediction from the distorted native conformation. J Comput Chem **15:**488–506. http://dx.doi.org/10.1002/jcc.540150503.
41. **Song J, Gao X, Galan JE.** 2013. Structure and function of the Salmonella Typhi chimaeric A_2B_5 typhoid toxin. Nature **499:**350–354. http://dx.doi.org/10.1038/nature12377.
42. **Barouch DH, Yang ZY, Kong WP, Korioth-Schmitz B, Sumida SM, Truitt DM, Kishko MG, Arthur JC, Miura A, Mascola JR, Letvin NL, Nabel GJ.** 2005. A human T-cell leukemia virus type 1 regulatory element enhances the immunogenicity of human immunodeficiency virus type 1 DNA vaccines in mice and nonhuman primates. J Virol **79:**8828–8834. http://dx.doi.org/10.1128/JVI.79.14.8828-8834.2005.
43. **Reeves PJ, Callewaert N, Contreras R, Khorana HG.** 2002. Structure and function in rhodopsin: high-level expression of rhodopsin with restricted and homogeneous N-glycosylation by a tetracycline-inducible N-acetylglucosaminyltransferase I-negative HEK293S stable mammalian cell line. Proc Natl Acad Sci U S A **99:**13419–13424. http://dx.doi.org/10.1073/pnas.212519299.
44. **Seaman MS, Janes H, Hawkins N, Grandpre LE, Devoy C, Giri A, Coffey RT, Harris L, Wood B, Daniels MG, Bhattacharya T, Lapedes A, Polonis VR, McCutchan FE, Gilbert PB, Self SG, Korber BT, Montefiori DC, Mascola JR.** 2010. Tiered categorization of a diverse panel of HIV-1 Env pseudoviruses for assessment of neutralizing antibodies. J Virol **84:**1439–1452. http://dx.doi.org/10.1128/JVI.02108-09.
45. **Li M, Gao F, Mascola JR, Stamatatos L, Polonis VR, Koutsoukos M, Voss G, Goepfert P, Gilbert P, Greene KM, Bilska M, Kothe DL, Salazar-Gonzalez JF, Wei X, Decker JM, Hahn BH, Montefiori DC.** 2005. Human immunodeficiency virus type 1 env clones from acute and early subtype B infections for standardized assessments of vaccine-elicited neutralizing antibodies. J Virol **79:**10108–10125. http://dx.doi.org/10.1128/JVI.79.16.10108-10125.2005.
46. **Sanders RW, Derking R, Cupo A, Julien JP, Yasmeen A, de Val N, Kim HJ, Blattner C, de la Pena AT, Korzun J, Golabek M, de Los Reyes K, Ketas TJ, van Gils MJ, King CR, Wilson IA, Ward AB, Klasse PJ, Moore JP.** 2013. A next-generation cleaved, soluble HIV-1 Env trimer, BG505 SOSIP.664 gp140, expresses multiple epitopes for broadly neutralizing but not non-neutralizing antibodies. PLoS Pathog **9:**e1003618. http://dx.doi.org/10.1371/journal.ppat.1003618.
47. **Julien JP, Lee JH, Cupo A, Murin CD, Derking R, Hoffenberg S, Caulfield MJ, King CR, Marozsan AJ, Klasse PJ, Sanders RW, Moore JP, Wilson IA, Ward AB.** 2013. Asymmetric recognition of the HIV-1 trimer by broadly neutralizing antibody PG9. Proc Natl Acad Sci U S A **110:**4351–4356. http://dx.doi.org/10.1073/pnas.1217537110.
48. **Totrov M, Jiang X, Kong XP, Cohen S, Krachmarov C, Salomon A, Williams C, Seaman MS, Abagyan R, Cardozo T, Gorny MK, Wang S, Lu S, Pinter A, Zolla-Pazner S.** 2010. Structure-guided design and immunological characterization of immunogens presenting the HIV-1 gp120 V3 loop on a CTB scaffold. Virology **405:**513–523. http://dx.doi.org/10.1016/j.virol.2010.06.027.
49. **Zolla-Pazner S, Cohen SS, Krachmarov C, Wang S, Pinter A, Lu S.** 2008. Focusing the immune response on the V3 loop, a neutralizing epitope of the HIV-1 gp120 envelope. Virology **372:**233–246. http://dx.doi.org/10.1016/j.virol.2007.09.024.
50. **Zolla-Pazner S, Kong XP, Jiang X, Cardozo T, Nadas A, Cohen S, Totrov M, Seaman MS, Wang S, Lu S.** 2011. Cross-clade HIV-1 neutralizing antibodies induced with V3-scaffold protein immunogens following priming with gp120 DNA. J Virol **85:**9887–9898. http://dx.doi.org/10.1128/JVI.05086-11.
51. **Wang S, Pal R, Mascola JR, Chou TH, Mboudjeka I, Shen S, Liu Q, Whitney S, Keen T, Nair BC, Kalyanaraman VS, Markham P, Lu S.** 2006. Polyvalent HIV-1 Env vaccine formulations delivered by the DNA priming plus protein boosting approach are effective in generating neutralizing antibodies against primary human immunodeficiency virus type 1 isolates from subtypes A, B, C, D and E. Virology **350:**34–47. http://dx.doi.org/10.1016/j.virol.2006.02.032.
52. **Pissani F, Malherbe DC, Schuman JT, Robins H, Park BS, Krebs SJ, Barnett SW, Haigwood NL.** 2014. Improvement of antibody responses by HIV envelope DNA and protein co-immunization. Vaccine **32:**507–513. http://dx.doi.org/10.1016/j.vaccine.2013.11.022.
53. **Upadhyay C, Mayr LM, Zhang J, Kumar R, Gorny MK, Nadas A, Zolla-Pazner S, Hioe CE.** 2014. Distinct mechanisms regulate exposure of neutralizing epitopes in the V2 and V3 loops of HIV-1 envelope. J Virol **88:**12853–12865. http://dx.doi.org/10.1128/JVI.02125-14.
54. **Morales JF, Morin TJ, Yu B, Tatsuno GP, O'Rourke SM, Theolis R, Jr, Mesa KA, Berman PW.** 2014. HIV-1 envelope proteins and V1/V2 domain scaffolds with mannose-5 to improve the magnitude and quality of protective antibody responses to HIV-1. J Biol Chem **289:**20526–20542. http://dx.doi.org/10.1074/jbc.M114.554089.
55. **Kayman SC, Wu Z, Revesz K, Chen H, Kopelman R, Pinter A.** 1994. Presentation of native epitopes in the V1/V2 and V3 regions of human immunodeficiency virus type 1 gp120 by fusion glycoproteins containing isolated gp120 domains. J Virol **68:**400–410.
56. **McKeating JA, Shotton C, Jeffs S, Palmer C, Hammond A, Lewis J, Oliver K, May J, Balfe P.** 1996. Immunogenicity of full-length and truncated forms of the human immunodeficiency virus type I envelope glycoprotein. Immunol Lett **51:**101–105. http://dx.doi.org/10.1016/0165-2478(96)02562-X.
57. **Sok D, van Gils MJ, Pauthner M, Julien JP, Saye-Francisco KL, Hsueh J, Briney B, Lee JH, Le KM, Lee PS, Hua Y, Seaman MS, Moore JP, Ward AB, Wilson IA, Sanders RW, Burton DR.** 2014. Recombinant HIV envelope trimer selects for quaternary-dependent antibodies targeting the trimer apex. Proc Natl Acad Sci U S A **111:**17624–17629. http://dx.doi.org/10.1073/pnas.1415789111.
58. **Morales JF, Yu B, Perez G, Mesa KA, Alexander DL, Berman PW.** 2016. Fragments of the V1/V2 domain of HIV-1 glycoprotein 120 engineered for improved binding to the broadly neutralizing PG9 antibody. Mol Immunol **77:**14–25. http://dx.doi.org/10.1016/j.molimm.2016.07.003.